MODELING OF A MEMBRANE BASED HUMIDIFIER FOR FUEL CELL APPLICATIONS SUBJECT TO END-OF-LIFE CONDITIONS

Mads Pagh Nielsen[1] and Anders Christian Olesen
Aalborg University
Department of Energy Technology
9220 Aalborg, Denmark

Alan Menard
Dantherm Power A/S
9500 Hobro, Denmark

ABSTRACT

Proton Exchange Membrane (PEM) Fuel Cell Stacks efficiently convert the chemical energy in hydrogen to electricity through electrochemical reactions occurring on either side of a proton conducting electrolyte. This is a promising and very robust energy conversion process which can be used in many applications. For instance for automotive applications and various backup power systems substituting batteries. Humidification of the inlet air of PEM fuel cell stacks is essential to obtain optimum proton conductivity. Operational humidities of the anode and cathode streams having dew points close to the fuel cell operating temperature are required. These conditions must be met at the Beginning-Of-Life (BOL) as well as at the End-Of-Life (EOL) of the fuel cell system. This paper presents results of a numerical 1D model of the heat- and mass transport phenomena in a membrane humidifier with a Nafion-based water permeable membrane. Results are presented at nominal BOL-conditions and extreme EOL-conditions. A detailed sub-model incorporating the water absorption/desorption kinetics of Nafion and a novel and accurate representation of the diffusion coefficient of water in Nafion was implemented. The modeling explains why Nafion fails as a water permeable membrane at typical EOL-conditions.

Keywords: PEM fuel cell systems, Membrane Humidifiers, Nafion water diffusion, Numerical modeling.

NOMENCLATURE

a	Water activity, [-]
c_p	Specific heat capacity [J/(kg·K)]
D	Diffusion coefficient [cm²/s]
f_v	Volumetric membrane H_2O content, [-]
h_L	Latent specific enthalpy, [J/kg]
M	Dry molar mass of Nafion [kg/kmol]
m	Number of discretization points [-]
$\dot{m}$	Mass flow [kg/s]
$\dot{n}$	Molar flux [mole/s·m^2]
p	Total pressure [bar]
t	Thickness of Nafion membrane [m]
T	Temperature [K]
U	Total heat transfer coeff., [W/m^2*K]
V	Partial molar volume, [kmol/m^3]
$\dot{V}$	Volume flow [m^3/s]
ΔA	Area element in humidifier [m^2]
$\Delta\dot{m}$	Water mass flow exchanged [kg/s]
σ	Proton conductivity of Nafion [S/cm]
ρ	Density [kg/m^3]
ϕ	Surface roughness parameter [m/m]
λ	Nafion H_2O content [molH_2O/molSO_3^-]
ω	Absolute humidity [kg H_2O/kg dry air]

Subscripts

Air	Properties related to humid air
Dry	Ref. to dry stream/dry Nafion
Equil	Equilibrium membrane water cont.
H_2O	Water
i	Index in space
in	Inlet
out	Outlet
Membrane/M	Referring to the Nafion Membrane
Water/W	Properties related to water
Wet	Referring to the wet stream

[1] Corresponding author: Phone +45 9940 9259 E-mail: mpn@et.aau.dk

INTRODUCTION

A Proton Exchange Membrane (PEM) fuel cell stack provides high efficient energy conversion. A typical PEM fuel cell assembly is illustrated in figure 1 (left). A fuel cell stack consists of a number of serially connected cells configured in this way. Hydrogen, air and cooling water are supplied through manifolds in the longitudinal dimension of the fuel cell stack. The proton exchange membrane fuel cell principle (the membrane assembly or MEA) is illustrated in figure 1 (right) along with the chemical reactions taking place in the catalyst layers at either side of the electrolyte. Please note that the figure to the right is not in scale but is stretched in the through-MEA axial direction (GDL=Gas Diffusion Layer).

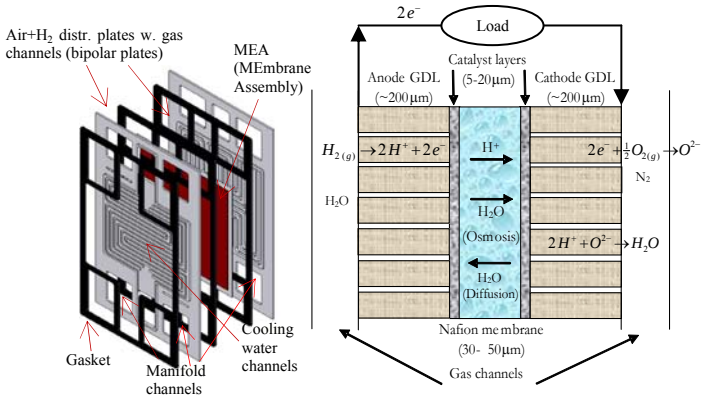

Figure 1: Typical PEM fuel cell assembly (left), PEM MEA topology and reactions (right).

The porous GDL assists the efficient distribution of reactants over the catalyst layers. Hydrogen is dissociated into protons and electrons at the anode. The electrons are passed through an electrical load. At the cathode, the electrons react with oxygen in the air and are reduced to O^{2-} ions which are combined with the protons passing the electrolyte membrane to produce water. A state-of-the-art single PEM fuel cell can operate at a potential of approximately 0.7 V at a current density of about 0.8 A/cm^2 MEA-area.

Humidifiers for PEM fuel cell stacks are essential components in order to reach acceptable performance and operational life. PEM fuel cells utilize Nafion membranes or polymers with similar properties. Nafion is a material which is a perfluorosulfonic acid PTFE (Poly-Tetra-Fluoro-Ethylene) copolymer. This PTFE, also known commercially as Teflon, is highly resistant to chemical reactions, due to the presence of strong carbon fluorine bonds. Thus, rugged polymer membranes can be manufactured thinner than 50 µm [1]. Hydrophilic sulfonic acid groups and their volume expanding nature absorbing water provides Nafion with the proton exchange properties.

However, the Nafion electrolyte membranes in PEM fuel cells must be fully hydrated with water in order to act as efficient proton conductors.
The specific proton conductivity in S pr. cm membrane thickness as function of water activity (i.e. partial pressure of water divided by saturation pressure of water at a given temperature) or relative humidity (as this is often referred to in the case of humid air up to activities of 1) of the fuel cell membrane is shown in figure 2.

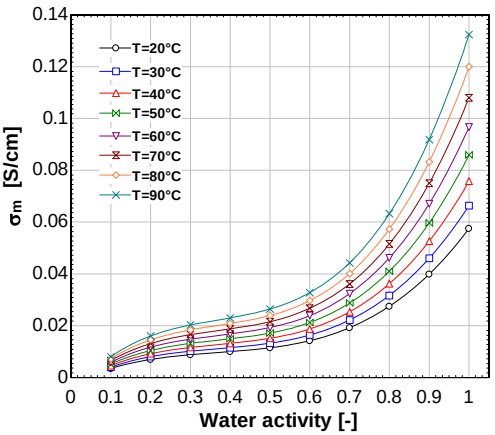

Figure 2: Nafion H^+ conductivity vs. activity & temperature.

It is thus essential, that the reactant gasses supplied to the PEM fuel cell stack (on both the anode and cathode) are humidified so that the membrane relative humidity is close to unity where optimum conductivity is achieved. At water activities exceeding 1, there is a risk of flooding the porous catalyst layers in the fuel cell stack.

Through the electrochemical conversion in a fuel cell, the reactants (hydrogen and oxygen) are converted to water. Membrane humidifiers offer the advantage of utilizing the product water in the depleted cathode exhaust air to humidify the dry inlet streams, simultaneously preheating the gas-

ses to the operational temperature of the fuel cell stack. Typically, the outlet air from the cathode is saturated with water at the operational temperature of the fuel cell stack (typically~60-70ºC). Either an air or a water cooling system makes sure that the stack temperature is maintained within a certain margin. The humidification is thus a balance of ensuring sufficient water to hydrate the electrolyte membrane, while simultaneously avoiding flooding of liquid water in the various parts of the fuel cell MEA [1].

A typical desired conditioning of the streams is to reach a dew point temperature of the dry air outlet (i.e. the humid air stream supplied to the fuel cell stack cathode inlet) from the humidifier close to the stack temperature. A schematic illustration of a typical fuel cell system configuration including a membrane humidifier is shown in figure 3.

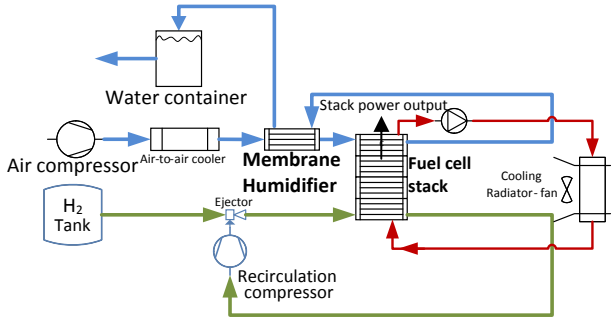

Figure 3: Humidifier integrated in a PEM-system.

At the fuel cell anode, hydrogen is supplied. The excess unreacted hydrogen leaving the anode is typically recirculated using an ejector often supplied by a small fan or compressor. The system is periodically purged to avoid problems with Nitrogen cross-over from the cathode side air [1]. Water is produced through the cathode half-reaction and typically, the higher water concentration here means that water migrates by back-diffusion from the cathode to the anode. By recirculating the anode output of hydrogen and water, active anode humidification is typically not necessary.

An air compressor supplies the air to the fuel cell stack cathode-side. Through the compression process, the temperature increases and thus the relative humidity and thus the water activity of the humid ambient air decrease significantly.

At EOL-conditions (normally after 10-20,000 hours of operation, depending on the application), the compressor efficiency has typically decreased meaning that the incoming air is further heated. Simultaneously, the fuel cell stack has also degraded affecting the operational conditions of the humidifier. An increased flow of both reactant gasses (air & H_2) to the fuel cell stack is necessary to maintain the required stack power output.

At very dry ambient conditions (for instance in a dessert with an ambient temperature of 50ºC) or conditions at higher altitudes at decreased pressures (for instance in the mountains), the temperature of the dry air inlet to the humidifier can be as high as 80ºC. A work-around to resolve this is to add an air-cooler after the air compression to cope with these EOL-extreme-conditions but this component adds to system cost and complexity.

In this paper, a nominal BOL-case and an EOL-case with realistic conditions are considered to model the humidifier behavior.

Membrane humidifiers have been utilized as the predominant means of humidification in commercial fuel cell stack systems during the past decade. The principle of utilizing the wet and warm depleted air exiting the cathode was first demonstrated in a 2kW stack setup developed by the Paul Scherrer Institute in 1999. Later membrane humidification has been adapted as the dominant method of humidification in PEM-systems by most system integrators [2-12]. Typically, membrane humidifiers are designed as shell and tube heat and mass exchangers (see figure 4) with a number of Nafion tubes (in the shell there are a bundle of fibers/tubes with inner-diameters of typically 0.4-0.8 mm).

Figure 4: Shell and tube membrane humidifier.

Recently, the trend has been going towards using circular tube shaped membranes based on Nafion

and polymers with similar properties due to their good mechanical, gas sealing properties and good water transport properties. Consequently, Nafion in fuel cell systems serves the different purposes as a water and proton conductor in PEM's and furthermore as water conductor in the humidifiers. This paper presents a 1D distributed parameter steady-state model of a membrane humidifier.

DIFFUSION OF WATER IN NAFION

The water transport in Nafion has been extensively researched [13-17]. The transport process is mainly governed by the water diffusivity D_w of the membrane subject to different conditions. Water diffusion coefficients in Nafion based on different sources are illustrated in figure 5 as function of the Nafion water content λ (a value of 14 corresponds to a fully hydrated membrane. Values > 14 indicate the presence of liquid water).

The different research groups determining these water diffusion coefficients measured the diffusion coefficient at very different conditions with varying methods. Some of the apparent deviations can be explained strictly mathematically as pointed out in [13]. The peaking diffusion coefficients around 3 from some references could very well be due to mathematical artifacts. If liquid water is present, the diffusion coefficient increases further.

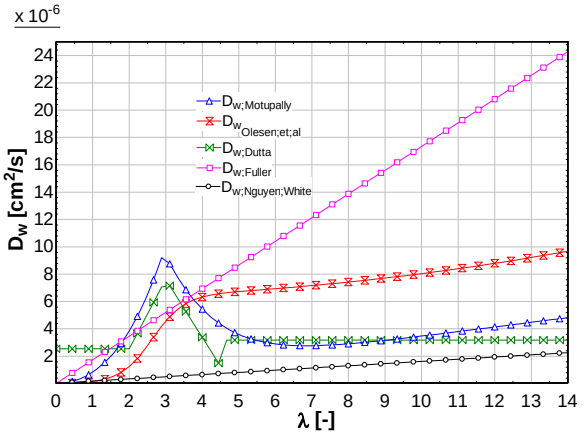

Figure 5: D_w as function of λ [13-17].

The recent relations proposed by Olesen et al. [13] are used for the calculation of the water diffusion through the membrane. These equations, account for the water uptake and release kinetics of Nafion, while additionally also accounting for the swelling of the membrane. What is notable, using this model, is that a low λ results in virtually no water transport when kinetics is accounted for [13]. D_W's below 5 strongly limits water transport.

To model the sorption/desorption kinetics of water in the Nafion membrane, the model suggested by Ge et al. [21] has been used. This paper suggests a non-equilibrium formulation of the water sorption/desorption phenomena. Equation (1) and (2) govern the kinetics of water sorption/desorption:

$$\dot{n}_{H_2O,membrane} = \phi k \frac{\rho_{membrane}}{M_{membrane}} \left(\lambda - \lambda_{equil}\right) \tag{1}$$

$$k = k^{T_0} f_v \exp\left(2416\left(\frac{1}{303} - \frac{1}{T}\right)\right) \tag{2}$$

In (1) ϕ is a factor to account for the actual surface roughness. In [13] it is suggested to use a value of unity. The factor k^{T_0} is 1.14 m/s in case of absorption and to 4.59 m/s in case of desorption [21].

From [13], it can be found that the volumetric membrane water content is:

$$f_v = \frac{\lambda V_w}{\left(\frac{M_{membrane}}{\rho_{membrane}} + \lambda \cdot V_w\right)} \tag{3}$$

The partial molar volume of water V_w is found from (4) accounting for membrane water swelling:

$$1 + 0.0126 \cdot \lambda = 1 + \left(\frac{V_w}{\left[\frac{M_{membrane}}{\rho_{membrane}}\right]}\right) \cdot \lambda \tag{4}$$

The through-membrane molar flux of water is:

$$\dot{n}_{H2O;membrane} = \left(\frac{\rho_{Nafion;dry}}{M_{Nafion;dry} \cdot t_{membrane}}\right) \cdot \int_{\lambda_{dry}}^{\lambda_{wet}} D_w \, d\lambda \tag{5}$$

Equating equations (1) and (5), makes it possible to calculate the actual water content in the membrane based on the above kinetic model.
Based on the work presented in [13], following empirical fit for the diffusion coefficient of water in Nafion at different temperatures was found:

$$D_w = \left(5.39 \times 10^{-2} + 1.455 \times 10^{-5} \cdot \lambda^2\right) \cdot \left(1 + tanh\left(\frac{\lambda - 2.6225}{0.8758}\right)\right) \cdot exp\left(-\frac{3343}{T}\right) \tag{6}$$

Here λ as function of water activity is found from the references [13 & 14]:

$$\lambda = \begin{cases} 0.043 + 17.81a - 39.85a^2 + 36.0a^3 & ,0 \le a \le 1 \\ 14 + 1.4(a-1) & ,1 < a \le 3 \end{cases} \quad (7)$$

Multiplying the molar flux of water through the membrane by the Nafion membrane area and the molar mass of water enables us to find the water mass flow exchanged through the membrane, $\Delta\dot{m}$.

EXPERIENCES FROM FIELD TESTS

Several commercial Nafion-based membrane humidifiers were tested in fuel cell systems subject to real-life conditions by the Danish fuel cell system manufacturer Dantherm Power A/S.

Tests were conducted at different conditions on a commercial 3kW Ballard® PEM fuel cell stack system reflecting expected EOL stack conditions and extreme ambient conditions. The tests showed that the humidifiers would work at nominal conditions at BOL but would fail at high ambient temperatures at EOL due to limited water transport.

MODELING FORMULATION

A numerical model was developed to understand this phenomenon and to investigate how to optimize the system to be able to handle these extreme conditions at the lowest possible cost. The model was based on the same conditions as used in the abovementioned tests. The following inlet and outlet conditions were studied for the 2 cases:

Nominal BOL Case:
Humidifier Nafion tube total surface area: 0.5 m^2
Humidifier (dry side) inlet temperature: 45ºC
Humidifier (dry side) inlet pressure: 1.145 bar
Humidifier (wet side) inlet temperature: 70ºC
Humidifier (wet side) inlet pressure: 1.1 bar
Relative humidity at humidifier dry inlet: 14%
Relative humidity at humidifier wet inlet: 100%
Flow (on either side of humidifier) ~ 170 NLPM

Extreme EOL Case:
Humidifier Nafion tube total surface area: 0.5 m^2
Humidifier (dry side) inlet temperature: 80ºC
Humidifier (dry side) inlet pressure: 1.145 bar
Humidifier (wet side) inlet temperature: 70ºC
Humidifier (wet side) inlet pressure: 1.1 bar
Relative humidity at humidifier dry inlet: 0%
Relative humidity at humidifier wet inlet: 100%
Flow (on either side of humidifier) ~ 180 NLPM

The modeling was performed in the tool Engineering Equation Solver (EES) [22]. EES solves a set of non-linear equations using an efficient and accurate modified reduced step-size Newton-Raphson solver and has built-in thermo-physical property relations including psychrometric functions for the properties of humid air. In the modeling, it is assumed that the humid air will properly reflect the actual conditions with oxygen-depleted air due to the similarities of oxygen and nitrogen.

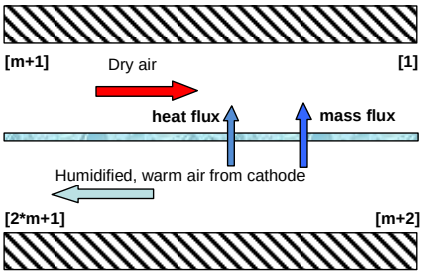

Figure 6: Modeling domain of the humidifier.

The steady power and mass flow balances in eqs. (8)-(11) were setup for the humidifier, using a discretized non-linear algebraic equation form where $i \in [1..m]$. It is modeled as a 1D heat and mass exchanger with m elements (here the wet stream power balance (8) is referring to the hot and wet stream exiting the cathode of the fuel cell stack and the dry stream energy balance (9) is the air stream entering counter current to be humidified. (10) and (11) give the mass flow balances).

$$\Delta\dot{m}_{water,\mathrm{m-i+1}} \cdot h_l = \rho_{wet} \cdot c_{p,\mathrm{wet,air}} \cdot \dot{V}_{wet} \cdot \left[T_{i+1} - T_i\right] + U \cdot \Delta A \cdot \left[T_{i+m+1} - T_i\right] \quad (8)$$

$$\Delta\dot{m}_{water,i} \cdot h_l = U \cdot \Delta A \cdot \left[T_{i+m+2} - T_{i+1}\right] - \rho_{dry} \cdot c_{p,\mathrm{dry}} \cdot \dot{V}_{dry} \cdot \left[T_{i+m+1} - T_{i+m+2}\right] \quad (9)$$

$$\dot{m}_{dry,i} = \dot{m}_{dry,i+1} + \Delta\dot{m}_{water,i} \quad (10)$$

$$\dot{m}_{\mathrm{wet},i+m+2} = \dot{m}_{\mathrm{wet},i+m+1} - \Delta\dot{m}_{water,\mathrm{m-i+1}} \quad (11)$$

The equidistant grid for the numerical calculations is arranged in a vector so that the inlet of the dry stream is at index [m+1], the inlet of the wet

stream at index [m+2], the outlet of the dry stream is [1] and the outlet of the wet stream is [2*m+1] (see figure 6).

Thermal and calorimetric properties were calculated in each element based on the thermophysical library in EES. Heat transfer-wise; there is laminar flow in all channels on both the shell and the tube side leading to constant Nusselt numbers. Appropriate values for circular tubes (tube side~3.66) and ~triangular tubes (shell side~2.47) were used to approximate the overall heat transfer coefficient [19].

The thermal conductivity of Nafion has been neglected. It depends on the water content in the Nafion and has been measured in several studies (for example in [23] & [24]). Even in cases of no hydration, the thermal conductivity is negligible.

It was furthermore assumed that the system is well-insulated, so surface heat losses are neglected. The flow distributions in tubes on either side were found to be quite even between the fibers in the shell-and-tube topologies under the given conditions [5]. Flow mal-distribution has thus been neglected on as well the shell as the tube side of the membrane humidifier.

The pressure losses in the humidifier channels were measured to be around 10-30 mbar at the earlier mentioned flow conditions. The pressure loss in the stack ranges from 10-20 mbar. An average pressure loss has been included as seen in the inlet and outlet conditions used in modeling.

Depending on the degree of condensing and surface evaporation at either side, the last term in the numerator with h_l (latent energy contribution) can be positive or negative. In general the transport through Nafion occurs via a so-called pervaporation process [20], which means that no direct latent energy is involved in the transport process through the membrane. However, surface evaporation will be present and in some cases condensation will occur (at water activities exceeding 1). These effects have been included in the calculation of the calorimetric properties in the membrane humidifier.

A grid consistency study showed that a discretization with 60 elements was sufficient to reach consistent results. Overall, this resulted in a non-linear equation set with approximately 3000 equations and 3000 unknowns. Energy and mass balances were calculated indicating energy and mass defects of far less than 1% in all calculated cases.

RESULTS AND DISCUSSION

Modeling results for the humidifier temperatures in counter-current operation mode are illustrated in figure 7.

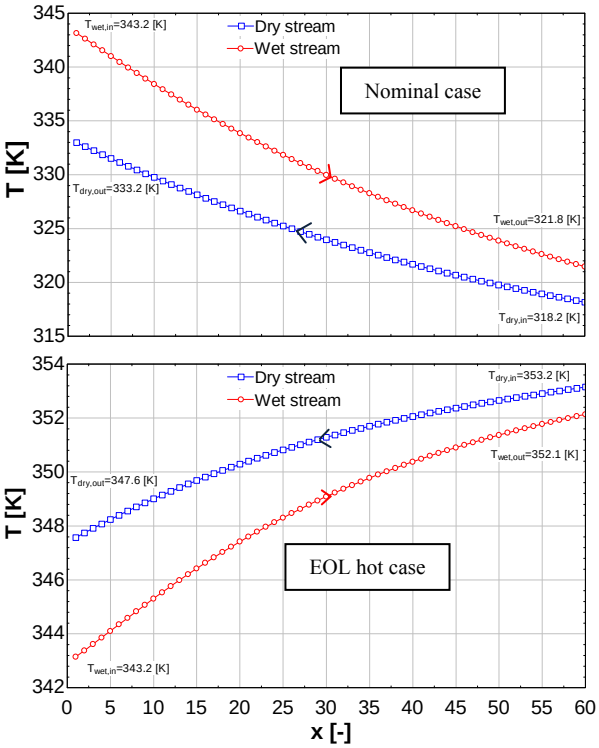

Figure 7: Temperature profiles in humidifier.

In the nominal BOL-case, there will be condensation at the wet stream outlet as the water activity exceeds 1.

The plots in figure 8 show the variation of the water activity (i.e. the ratio between the partial pressure of water in the humid air divided by the saturation pressure at the given temperature) along with the dry stream temperature in the 60 elements the two sides was discretized into through the humidifier (note the location of inlets and outlets).

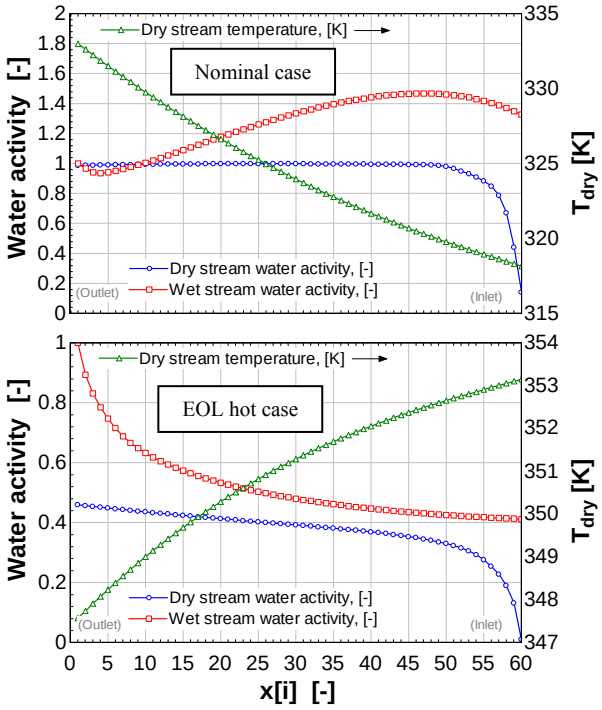

Figure 8: Water activities and dry stream temp.

The stack inlet temperature is desired to be 60ºC and the outlet temperature is ~70ºC. It follows from figure 8 that the membrane humidifier works properly at the nominal BOL-case where it saturates the cathode air with water ideally at a temperature close to the desired inlet temperature. At the extreme EOL conditions, the humidifier fails to reach the desired water transfer. This contradicts theoretical studies with other D_w-relations which indicate that the humidifier should work properly under such conditions. The present model agrees with the experiences from field tests.

The water contents in the two humidifier channels and the membrane are shown in figure 9. The reason for the bad water transport properties can be found considering these membrane water contents. In the nominal BOL-case, the membrane is nearly fully hydrated with water (i.e. λ~14). For the EOL extreme hot case, the water content is very low and when considering the sorption/desorption kinetics, there is only a very limited water transport through the membrane.

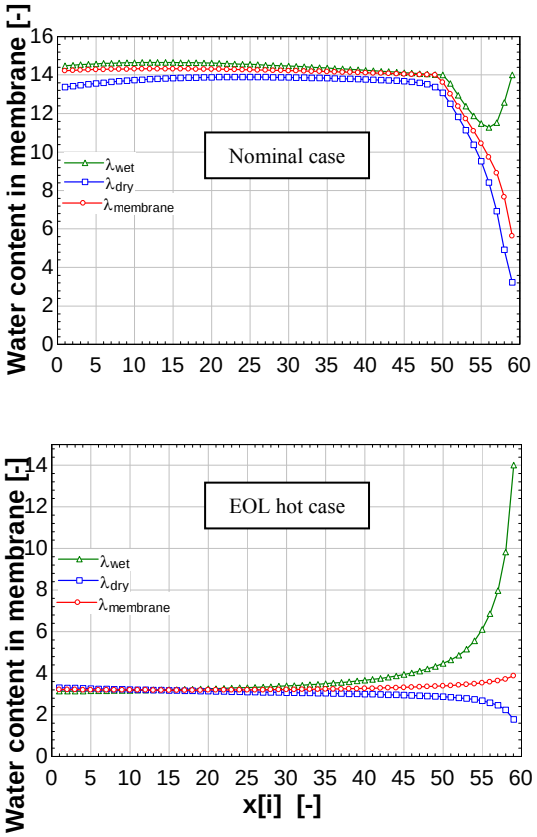

Figure 9: Membrane water contents.

Figure 10 and 11 are psychrometric charts illustrating the thermal processes occurring at respectively the dry and wet side of the humidifier. The psychrometric charts show the moist air (the property called "AirH_2O" in EES) absolute humidity or 'humidity ratio' as the ordinate in [kg water/kg dry air] and the abscissa is the temperature in [K]. The upper thicker black curve shows the saturation line of water in dry air subject to these properties (corresponding to a relative humidity of 100%~an activity of 1). The lines below from 0.2-0.8 illustrate iso-lines of relative humidity from 20-80%. Wet bulb temperatures and specific volumes are additionally given in the charts.

The two charts in figure 10 show the process in the nominal BOL-case. It is worth noting, that the nominal BOL-case reaches equilibrium at the saturation line (relative humidity of 100%).

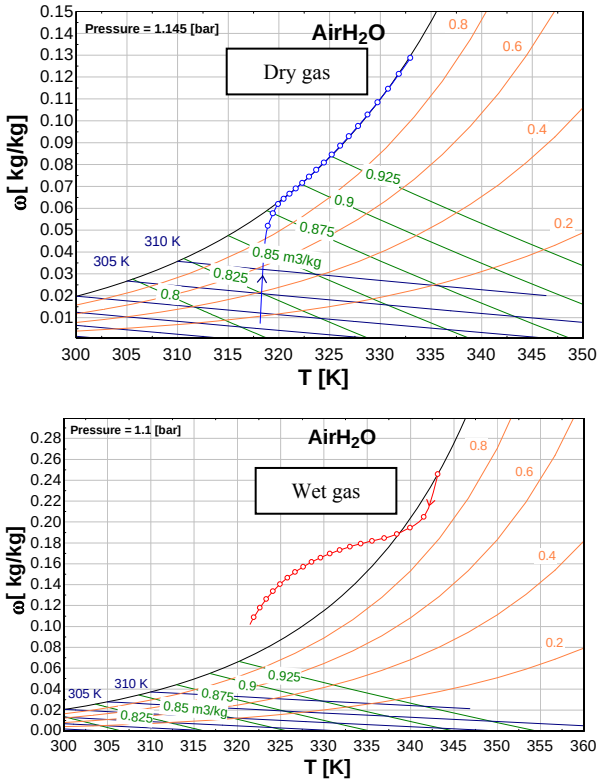

Figure 10: BOL case in psychrometric charts.

The plots in figure 11 illustrate the psychrometric charts for the extreme EOL case – i.e. operation with worn system components and extremely dry and warm conditions.

In this case, no equilibrium is reached but the absolute humidity keeps increasing slightly while the temperature decreases. Increasing the area of the humidifier will clearly not solve this problem. A certain degree of cooling will be required. In this case, the critical issue is not the dry ambient air but rather the high temperature resulting in a very low water activity at the dry air inlet to the humidifier limiting the mass transfer of water.

Figure 12 illustrates the transport of water through the membrane in two cases. The overall mass flow rate of water transported through the Nafion tubes of the humidifier are found by integrating the curves to yield respectively 0.47 g/s for the BOL nominal case and 0.35 g/s for the EOL extreme case. The difference may appear to be quite small but the fuel cell stack cannot operate at 0.35 g/s.

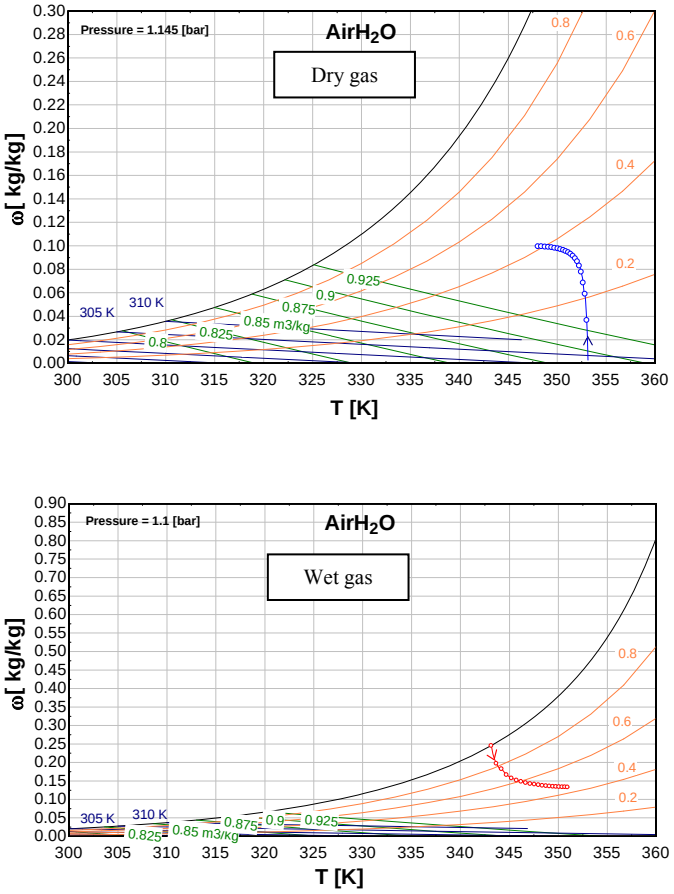

Figure 11: EOL case in psychrometric charts.

The membrane water transport from the wet to the dry side of the humidifier shows that the area of the membrane in many cases is less important in terms of water transfer as the majority of the mass transport will take place over a very limited area of the Nafion-membrane-tubes in the humidifier. This leaves a potential for constructing part of the tubes with a cheaper material having acceptable heat transfer properties. Nafion is a quite expensive material, so this is a quite relevant issue.

The streams must also be heated to the stack temperature so the heat transfer area is required.

In some cases, when operating the system at warm EOL conditions, it might be beneficial to bypass part of the insulated membrane humidifier area, since this leads to a better water transfer in this particular case if the humid air could be cooled in

an intelligent way not requiring additional components.

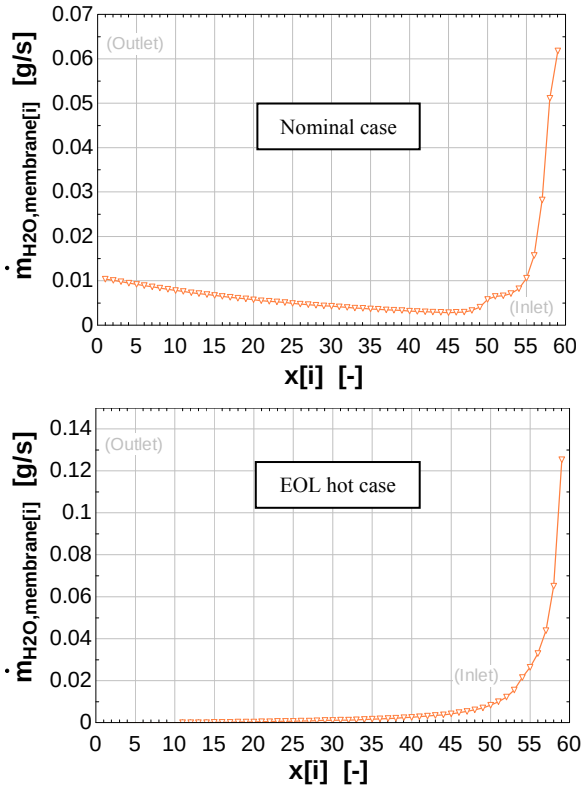

Figure 12: Nafion membrane water transport.

CONCLUSION

A steady-state distributed parameter model of a membrane humidifier has been developed. It has been found that the present simplified 1D-modeling approach has been able to replicate the physical phenomena and trends occurring during real life conditions in membrane humidifiers quite well. It is believed that the model with further improvements and comparison with more detailed experiments can be a very useful tool when designing and optimizing membrane based humidifiers for PEM fuel cell applications.

Future work will include the investigation of the influence of dynamic phenomena in the water transport process and a further study of the two-phase effects in membrane humidifiers.

ACKNOWLEDGEMENT

This work has been funded through the EUDP programme project entitled "USDan, Fuel Flexible μCHP". We gratefully acknowledge the funding from the Danish Energy Authorities.

REFERENCES

[1] Bernardi D. M., Verbrugge M. W, *A Mathematical Model of the Solid Polymer-Electrolyte Fuel Cell*, J. Electrochem. Soc. 1992 139(9).

[2] Choi K. H, Park D. J., Rho Y. W., Kho Y. T., T.H Lee, *A study of the internal humidification of an integrated PEMFC stack*, Journal of Power Sources, Volume 74, Issue 1, Jul. 1998, 146-150.

[3] Bhatia D., Sabharwal M., Duelk C., *Analytical model of a membrane humidifier for polymer electrolyte membrane fuel cell systems*, International Journal of Heat and Mass Transfer, Volume 58, Issues 1–2, March 2013, Pages 702-717.

[4] Huizing R., Fowler M., Mérida W., Dean J., *Design methodology for membrane-based plate-and-frame fuel cell humidifiers*, Journal of Power Sources, Volume 180, Issue 1, 15 May 2008, Pages 265-275, ISSN 0378-7753

[5] Gabelman A., Hwang S., *Hollow fiber membrane contactors*, Journal of Membrane Science, Volume 159, Issues 1–2, 1 July 1999, P. 61-106.

[6] Park S., Choe S., Choi S., *Dynamic modeling and analysis of a shell-and-tube type gas-to-gas membrane humidifier for PEM fuel cell applications*, International Journal of Hydrogen Energy, Volume 33, Issue 9, May 2008, Pages 2273-2282.

[7] Kang S., Min K., Yu S., *Two dimensional dynamic modeling of a shell-and-tube water-to-gas membrane humidifier for proton exchange membrane fuel cell*, International Journal of Hydrogen Energy, Volume 35, Issue 4, February 2010, Pages 1727-1741.

[8] Chen D., Li W., Peng H., *An experimental study and model validation of a membrane humidifier for PEM fuel cell humidification control*, Journal of Power Sources, Volume 180, Issue 1, 15 May 2008, Pages 461-467.

[9] Zhang H., Qian Z., Yang D., Ma J., *Design of an air humidifier for a 5 kW proton exchange membrane fuel cell stack operated at elevated temperatures*, International Journal of Hydrogen Energy, Volume 38, Issue 28, 19 September 2013.

[10] Zhang L., Huang S., *Coupled heat and mass transfer in a counter flow hollow fiber membrane module for air humidification*, International Journal of Heat and Mass Transfer, Volume 54, Issues 5–6, February 2011, Pages 1055-1063.

[11] Cave P., Mérida W., *Water flux in membrane fuel cell humidifiers: Flow rate and channel location effects*, Journal of Power Sources, Volume 175, Issue 1, 3 January 2008, Pages 408-418.

[12] Kadylak D., Mérida W., *Experimental verification of a membrane humidifier model based on the effectiveness method*, Journal of Power Sources, Volume 195, Issue 10, 15 May 2010, Pages 3166-3175.

[13] Olesen A. C, Berning T, Kær S. K. *On the diffusion coefficient of water in polymer electrolyte membranes.* ECS Transactions, 2012; 50 (2) 979-991.

[14] Thomas A., Zawodzinski Jr., T., Springer F. U., Gottesfeld S., *Characterization of polymer electrolytes for fuel cell applications*, Solid State Ionics, Volume 60, Issues 1–3, March 1993, Pages 199-211, ISSN 0167-2738

[15] Motupally S., Becker A. J., Weidner J. W., *Diffusion of Water in Nafion 115 Membranes*, J. Electrochem. Soc. 2000 147(9): 3171-3177.

[16] Fuller T. F., Newman J., *Water and Thermal Management in Solid-Polymer-Electrolyte Fuel Cellsm,* J. Electrochem. Soc. 1993 140(5): 1218-1225.

[17] Nguyen T. V., White R. E., *A Water and Heat Management Model for Proton-Exchange-Membrane Fuel Cells*, J. Electrochem. Soc. 1993 140(8): 2178-2186.

[18] Dutta S., Shimpalee S., Van Zee J. W., *Numerical prediction of mass-exchange between cathode and anode channels in a PEM fuel cell*, International Journal of Heat and Mass Transfer, Volume 44, Issue 11, June 2001, Pages 2029-2042.

[19] Mills A. F. *Heat And Mass Transfer.* Richard D. Irvin Inc., 1995

[20] Duan Q., Wang H., Benziger J., *Transport of liquid water through Nafion Membranes*. Journal of Membrane Science. 88-94, 2011.

[21] Ge S., Li X., Yi B., Hsing, I. M., *Absorption, desorption, and transport of water in polymer electrolyte membranes for fuel cells*. Journal of Electrochemical Society, 152, A1149, 2005.

[22] URL of F-Chart Software, which is the company developing and selling Engineering Equation Solver (EES) http://fchart.com.

[23] Burheim O., Vie P. J. S., Pharoah J. G., Kjelstrup S. *Ex Situ measurements of through-plane thermal conductivities in a polymer electrolyte fuel cell.* Journal of Power Sources, 195, 249-256, 2010.

[24] Khandelwal M, Mench M. M. *Direct measurement of through-plane thermal conductivity and contact resistance in fuel cell materials.* Journal of Power Sources, 161, 1106-1115, 2006.